Forschungszentrum Karlsruhe
in der Helmholtz-Gemeinschaft

Wissenschaftliche Berichte
FZKA 7294

The Muon Charge Ratio
in Cosmic Ray Air Showers

H. Rebel, O. Sima, A. Haungs,
J. Oehlschläger, C. Manailescu,
C. Morariu, A. Patrascioiu
Institut für Kernphysik

März 2007

Forschungszentrum Karlsruhe

in der Helmholtz-Gemeinschaft

Wissenschaftliche Berichte

FZKA 7294

The muon charge ratio in cosmic ray air showers

H. Rebel, O. Sima[*], A. Haungs, J. Oehlschläger,
C. Manailescu[*], C. Morariu[*], and A. Patrascioiu[*]

Institut für Kernphysik

[*]Department of Physics, University of Bucharest, Romania

Abstract

Various aspects of studies of the charge ratio of cosmic ray muons are reviewed. In particular the muon charge ratio of the lateral muon density distributions in single EAS is considered by simulations, in context of recent proposals to measure this observable in coincidence with EAS observations. Effects of the hadronic interaction do not lead to significant differences of the total μ^+ and μ^- content, while differences of the azimuthal variation of the muon densities of opposite charges and the azimuthal variation of the muon charge ratio appear to be very much pronounced, dependent on the direction of EAS incidence. This is due the influence of the geomagnetic field which induces similar effects in radio emission from extended air showers.

Zusammenfassung

Das Ladungsverhältnis der Myonen in ausgedehnten Luftschauern

Es wird ein Überblick verschiedener Aspekte von Untersuchungen des Ladungsverhältnisses von Myonen der kosmischen Strahlung gegeben. Inbesondere wird das Verhältnis der Dichte von positiven zu negativen Myonen in der Lateralverteilung von ausgedehnten Luftschauern betrachtet, im Kontext mit neueren experimentellen Vorschlägen, diese Observable in Koinzidenz mit Luftschauer-Beobachtungen zu messen. Es stellt sich heraus, dass Unterschiede in der hadronischen Wechselwirkung kaum zu signifikanten Unterschieden im integrierten μ^+ und μ^- - Gehalt des Luftschauers führen, während jedoch die Unterschiede in der azimutalen Variation der Myondichte gegensätzlicher Ladung und die Variation des Ladungsverhältnisses recht ausgeprägt sind und von der Einfallrichtung des Schauers abhängen. Dies wird als Einfluß des geomagnetischen Feldes verstanden und in Einzelheiten demonstriert. Manche Effekte ähneln den Effekten, die bei der Radioemission von ausgedehnten Luftschauern beobachtet werden.

II

Contents

IV

1 Introduction

Primary cosmic rays are dominantly high-energy protons, alpha particles and heavier nuclei in a relative amount decreasing with the atomic number. When penetrating from the outer space into the Earth's atmosphere they initiate the development of a phenomenon called Extensive Air Showers (EAS) by multiple production of particles in cascading interactions of the primary particles with atmospheric nuclei. The produced secondary radiation establishes an essential feature of our natural environment. It affects material and biological substances and comprises a specific part of the natural radiation background. Its study is of relevance in various scientific problems. Photons, electrons and positrons are the most numerous secondary particles in an EAS event, and the muonic component contributes only to few percent in the single shower. However, at lower primary energies, which are dominating due to the steeply falling primary spectrum, or in case of very inclined showers the electromagnetic shower component gets completely absorbed during the travel through the atmosphere, while the muons ("penetrating component") survive the propagation through even larger slant depths. Hence the inclusive secondary radiation flux in the atmosphere comprises mainly muons (c. 80% with c.100 muons $s^{-1}m^{-2}sr^{-1}$ on sea level). The cosmic rays muons originate from decay of hadronic secondaries produced in particle cascades by primary cosmic rays:

$$\pi^\pm \to \mu^\pm + \nu_\mu(\overline{\nu}_\mu) \qquad 100.0\ \% \text{ (lifetime } 2.6\cdot10^{-2}\mu s)$$
$$K^\pm \to \mu^\pm + \nu_\mu(\overline{\nu}_\mu) \qquad 63.5\ \% \text{ (lifetime } 1.2\cdot10^{-2}\mu s)$$

The muons decay with a larger life time ($2.2\mu s$):

$$\mu^+ \to e^+ + \nu_e + \overline{\nu}_\mu$$
$$\mu^- \to e^- + \overline{\nu}_e + \nu_\mu$$

The ratio of positive to negative muons, the so-called muon charge ratio $R_\mu(\mu^+/\mu^-)$ is a significant quantity which reflects important features of the hadronic meson production in cosmic ray collisions [1,2] and can help to discern the primary mass composition [2,3]. It is also immediately obvious that the muon flux in the atmosphere is strongly related to the neutrino flux and that the muon charge ratio

$$R_\mu(\mu^+/\mu^-) \sim R(\nu_e/\overline{\nu}_e)$$

provides relevant information for neutrino anomaly. The atmospheric neutrino anomaly is the observation of Super-Kamiokande [4] and other experiments [5] that the ratio of muonic to electronic neutrinos is much smaller than the theoretical predictions, $R(\nu_\mu/\nu_e)_{observed}/R(\nu_\mu/\nu_e)_{predicted} \ll 1$.
The deficit is interpreted in terms of neutrino flavour oscillations.

Several studies have re-examined the influence of the Earth's magnetic field on muon and neutrino fluxes [6,7]. At lower energies, the fluxes of the primaries and secondaries are influenced by the Earth's magnetic field, in particular by a magnetic rigidity cut-off of the primary cosmic rays penetrating the Earth's atmosphere from the cosmos [7], resulting in latitude dependence and in an East-West asymmetry of the incident flux [8]. There are numerous studies of the charge ratio of the atmospheric muon flux, on sea level (see the compilations [2, 9-11]) and also of the vertical dependence by balloon experiments e.g. [12-14]. They provide a highly inclusive information since the atmospheric flux is produced by many different EAS, with primary energies distributed along the steeply falling energy spectrum and the mass composition of the primary flux. When impinging on our Earths atmosphere they are additionally affected by the geomagnetic field. The influence of the geomagnetic field leads to a dependence of the muon charge ratio from the azimuth of the direction of incidence, in particular for low energy muons, which are dominantly originating of EAS at lower primary energies. The measured value of muon charge ratio which is empirically found to have a value of about 1.25 - 1.30, is mainly a result of the positive charge (proton) excess of the primary mass distribution, at $E_\mu > 10\,\text{GeV}$ slightly

increasing with the energy of the observed muons [11].

In the charge ratio of muons of single EAS (exclusive observations), which could be specified by a definite primary energy, the direction of incidence and eventually by the mass of the primary, the effects of the type of the hadronic interaction and geomagnetic field are expected to get revealed in a more pronounced way. In particular the lateral distribution of the EAS particles displays an azimuthal variation [15], which is influenced by the geomagnetic field, differently for μ^+ and μ^- and leading to an azimuthal variation of the charge ratio of the muon density distribution. In this communication we address the some aspects of the muon charge ratio, especially of the azimuthal variations of the muon density distribution, worked out by simulation studies. The considerations are in some context of recent proposals for studies of the muon charge ratio in single EAS, which will be observed with standard detector arrays as used (see ref. [16]) to study EAS.

2 Aspects of the hadronic interaction

Let us first to throw some light by the standard analytical approach of calculating the muon spectra and muon charge ratio of the atmospheric flux related to the hadronic interaction properties [17,18,19].
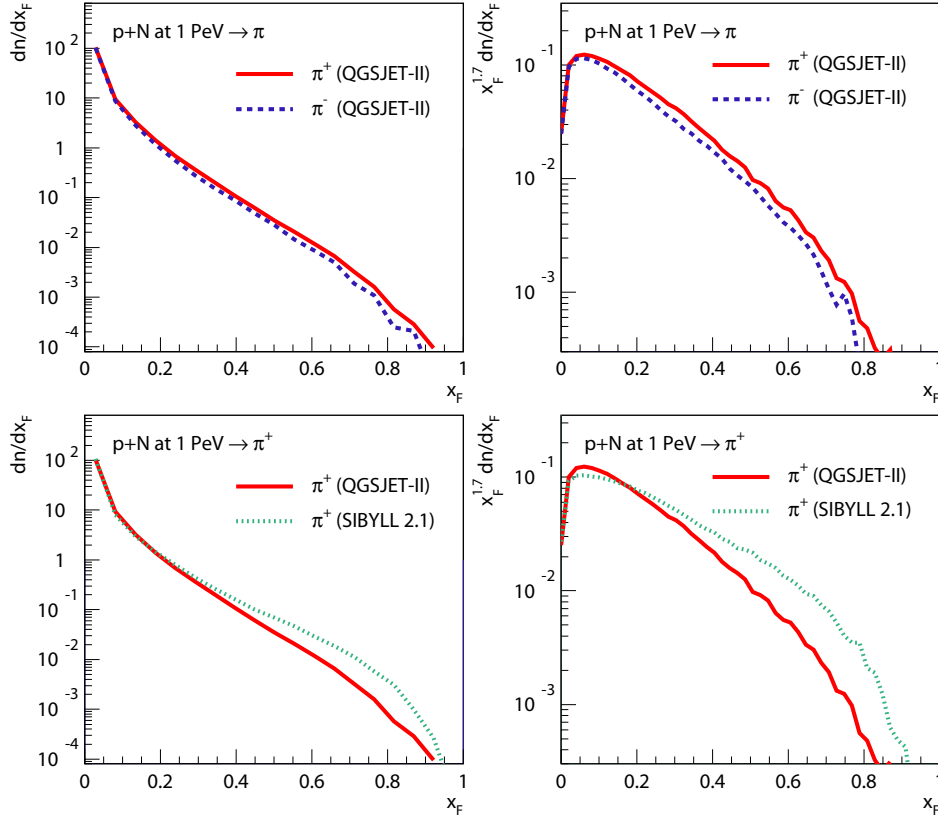

Figure 1: *Feynman x_F distributions dn/dx_F (left) and of the integrand of the energy-weighted moments $Z_{p\pi+}$ and $Z_{p\pi-}$ (right) for the positive and negative π in proton-nitrogen-collisions at an energy of $10^{15}eV$. Different hadronic interaction models [22,23] are compared (lower panel).*

In the approximation of the diffusion equations of the propagation of the particles through the atmosphere the fluxes of the particles are governed by the spectrum weighted moments Z of the inclusive cross sections

$$Z_{ac} = \int (x_F)^{\gamma-1} F_{ac}(x_F) \, dx_F \ ,$$

$$(x_F)^{\gamma-1} = (E_c/E_a)^{\gamma-1} \quad \text{relative energy transfer spectrum,}$$

$$F_{ac}(E_c, E_a) = E_c \, dn_c(E_c, E_a)/dE_c \ ,$$

dn_c = the number of particles c
produced in the energy bin dE_c,

$\gamma - 1$ = the power of the integral energy spectrum, $\gamma = 2.7$,

the indices a and c indicate the entrance and exit channels.

For the flux of pions und muons the moments $Z_{p\pi+/-}$ and $Z_{n\pi+/-}$ are of importance with the isospin symmetry
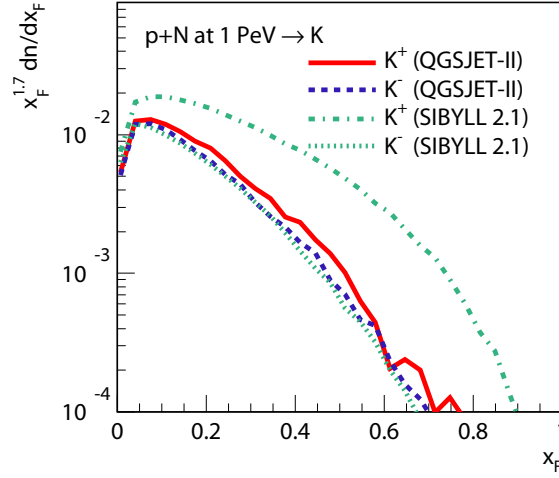
Figure 2: *Feynman x_F distributions of the integrand of Z_{pK} for positive and negative kaons, comparing QGSJET and SIBYLL predictions.*

$$Z_{p\pi+} = Z_{n\pi-} \, , \quad Z_{p\pi-} = Z_{n\pi+} \, .$$

As $Z_{p\pi+} > Z_{n\pi-}$ (see [18]) the value of the charge ratio does not just reflect the positive charge excess, but also the difference in the interaction producing pions of different charges. This is a consequence of the valence quark content of protons and pions. There are further source terms for the pion flux in the atmosphere represented by

$$Z_{\pi+\pi+} = Z_{\pi-\pi-} \quad \text{and} \quad Z_{\pi+\pi-} = Z_{\pi-\pi+} \, .$$

The contribution of subsequent pion interactions to the muon flux is affected by the decay probability of the π-mesons. At low energies the source of kaons are proton and neutron fluxes. The asymmetry in K^+- and K^--production is enhanced by $Z_{pK+} \neq Z_{nK-}$. K^+ and K^- do not belong to the same isospin multiplet since the $K^- = [s\bar{u}]$ does not have any contribution from the valence quark content of the incident nucleon, reflected by $Z_{pK+} \ll Z_{nK-} \approx Z_{pK-}$. Thus it is expected that the charge ratio of muons will increase at higher energies due to the enhanced contribution of the K^+ decay.

The approach, though applicable with some assumptions and approximations, is enabled by the fact that power law dependencies of the uncorrelated fluxes enter, and it has the advantage that measured inclusive cross sections could be introduced, as far they are known. Modern theoretical approaches of the muon flux and charge ratio start from Monte Carlo simulations of a sufficient number of single EAS events calculated along the primary energy spectrum and chemical distribution of cosmic rays (see [1] e.g.). The Monte Carlo simulations invoke as generators specific models of the hadronic interactions, which are reflected by the energy-weighted moments. Therefore measurements of the charge ratio are a source of information about the validity of such hadronic interaction models. In case of the atmospheric muons it has turned out that the results are rather stable against modifications of the models, except when higher energy muons would be considered. Michael Unger (L3 Collaboration) has put attention [20] that for muons with $E_\mu > 300\,GeV$ the charge ratio would be very discriminative, also due to the increasing influence of kaons. Such data of sufficient precision are actually missing (see also [21]). Accurate measurements, though requiring painstaking experimental patience, would be a challenging task of a detector installed in an underground laboratory.

The features of the particular models are revealed more distinctly, when the charge ratio of single showers is studied. Fig.1 compares the x_F-distributions of positive and negative π-mesons from proton collisions. Apparently there is an excess of positive pions

already in the single collision process, as mentioned above with explaining the observation of $Z_{p\pi+} > Z_{p\pi-}$ which leads already in a single shower to a value of $R_\mu(\mu^+/\mu^-) > 1$. Some exploratory calculations for proton induced EAS of $10^{15}eV$ find a μ^+-excess of less then about 10 % .

Since for atmospheric muons the single distribution is weighted by $(x_F)^{-1}$ and additionally mainly the primary energy range of $10^{12} - 10^{14}eV$ is of importance, a range of higher x_F values is contributing than for a single shower of $10^{15}eV$ where smaller x_F get dominating. Just for comparison fig.2 shows the x_F distributions for the kaons indicating the difference for kaons of opposite charges. The model dependence is well pronounced when comparing the results for QGSJET [22] and SIBYLL [23]. The difference between K^+- and K^--distributions may be underestimated in the QGSJET model and overestimated in the SIBYLL model (private communication by the authors of the models).

3   Geomagnetic effects of primary cosmic rays and EAS propagation

The observation of the influence of the geomagnetic field on cosmic rays has been published in 1933 [8]. The fluxes of positively charged primary cosmic rays that arrive the Earth's atmosphere comprise more particles travelling from West towards East than in the opposite direction and demonstrate that the dominant component of cosmic rays is positively charged. The feature is due to the magnetic field of the Earth, which does not allow that lowest rigidity particles (below a certain energy cut off) are able to reach the Earths surface. The East-West effect, whose detailed calculation has been discussed in several studies, e.g. in [1,7,24,25] is transferred to the secondary particles of air showers induced in the atmosphere, in particular to muons and to neutrinos [6,26,27]. Fig.3 displays schematically, how the different bending of the trajectories of positively and negatively charged muons by the geomagnetic field contributes to the East-West asymmetry of the muon charge ratio.
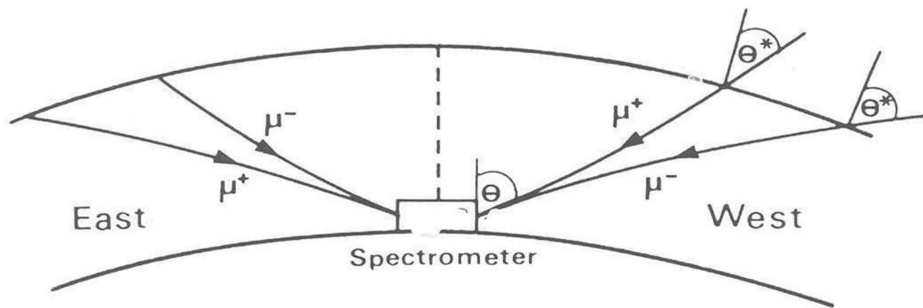

Figure 3: *Schematic explanation of the East-West effect of the charge ratio of atmospheric muons. The positive and negative muons observed with a spectrometer e.g. under a particular zenith angle Θ stem from different showers and different production directions due to the different magnetic bending of the muons of different charges. The magnetic bending of muons of different charges is different for muons travelling from East or from West, respectively. Thus different path lengths of muons change the decay probability and also the attenuation.*

The azimuthal variation of the muon charge ratio of atmospheric (inclusive) muons has been recently measured for low-energy muons for the latitude of the Bucharest (Romania) with a geomagnetic cut off of 5.6 GV [28]. The experimental findings agree well with theoretical predictions calculated by use of advanced procedures [1].

As indicated in Fig.3 apparently positively charged muons travelling towards East are bent "up" while bent "down", when travelling to West; for negative muons the situation is just opposite. Thus also in a single shower in presence of the geomagnetic field, positive and negative muons would bend in opposite directions perpendicular to the shower axis. The magnetic deviation would result in two separate centres of both muonic components.

In addition the muons of both components experience lateral dispersions arising from the transverse momenta and from multiple scattering and resulting in a distinct double-lobed pattern of the lateral distribution in the plane normal to the shower axis. The effect would depend on the direction of incidence and increases with the inclination of shower incidence i.e. when the distance of muon travel is increased due to the $\sec(\Theta)$ - dependence. Recently in view of the possibility to extract charge information of high energy EAS muons the geomagnetic effects on the shower development have been estimated in ref. [29,30] on basis of a modified Heitler model [31], originally known as "toy" model [32].

In the following section some results on the lateral muon distributions are presented resulting from extensive three-dimensional Monte Carlo simulations with reconstructions of the azimuthal variation of the muon component of inclined ($\Theta = 45°$) showers with the primary energies of 10^{14} eV and 10^{15} eV.

4   Azimuthal effects of lateral distributions of EAS muons

Azimuthal asymmetries and the azimuthal variation of the lateral distributions of charged EAS particles originate dominantly from the attenuation and geometrical effects of showers with inclined incidence. For a qualitative explanation we may assume that the EAS start from infinity and neglect any influence of the geomagnetic field in a first step of the argumentation. Thus we have cylindrical symmetry around the shower axis for all radial distances from the axis. For inclined showers hitting the observation plane, charged particles arriving first ("early" azimuthal EAS region) do experience less attenuation than the particles arriving later ("late" azimuthal EAS region), as the latter have travelled larger distances in atmosphere. The azimuthal asymmetries are also present when transforming the observed particle densities to the more relevant normal shower plane, orthogonal to the axis. Recently [15], in context of investigations of the charge particle EAS component, registered by the measurements of the KASCADE-Grande experiment [33], the azimuthal asymmetries have been demonstrated for EAS of inclined incidence of the primary energy range of 10^{17} eV.

An example is displayed in Fig. 4. It shows for a particular case of the direction of EAS incidence the azimuthal variation of the charge particle density for various (radial) distances from the shower centre in the plane normal to the shower axis and in the observation plane. For sake of convenient comparison the distributions for different radial distances have been normalized to the mean value of the charge particle densities at $\phi = 90°$ and $\phi = 270°$. These directions, corresponding to the intersection of the plane normal to the shower axis with the observation plane, were chosen for normalization because the attenuation effects are identical in both directions and also in the observation and in the normal plane. Here the (intrinsic) azimuth angles ϕ are counted counterclockwise from the direction of the intersection of the vertical plane containing the shower axis with the observation plane and the normal plane, respectively ($\phi = 0°$ corresponds to the "late" region of the shower).

The azimuthal dependence in the normal plane reflects mainly the effect of attenuation, while in the observation plane geometric effects are superimposed (points located in the observation plane at the same distance R from the shower core correspond to points located in the normal plane at distances from the core changing from $R \cdot \cos(\Theta)$ to R when ϕ changes from 0 to 90°).

In order to explore the azimuthal asymmetries of the lateral distributions, in particular of the muon component, some realistic and detailed Monte Carlo simulations of the EAS development have been performed. For the simulations the program CORSIKA [34] (version 6.5) has been used, invoking different models of the hadronic interaction, in particular QGSJET [22]. For particle interactions below $E_{lab} = 80$ GeV the GHEISHA option [35] is used. The earth magnetic field with a homogeneous field approximation, observation level and the particle energy thresholds have been chosen according to the conditions of the KASCADE-Grande experiment ($E_{\mu_{thres}} = 100$ MeV). The U.S. standard atmosphere (see [34]) has been adopted. For a realistic description the electron-photon component is simulated by the EGS option [36].

The performed simulations comprise proton and Fe induced EAS, with a zenith angle of incidence of $\Theta = 45°$ and arriving from different cardinal points: North, East, South, West. About 1000 showers have been simulated for most cases. For each event the muon lateral distributions for both muon charges separately and the distribution of the charge ratio of the muon density have been reconstructed. In order to explore the influence of the geomagnetic field, the simulations have been also done with the Earth's magnetic field switched off.

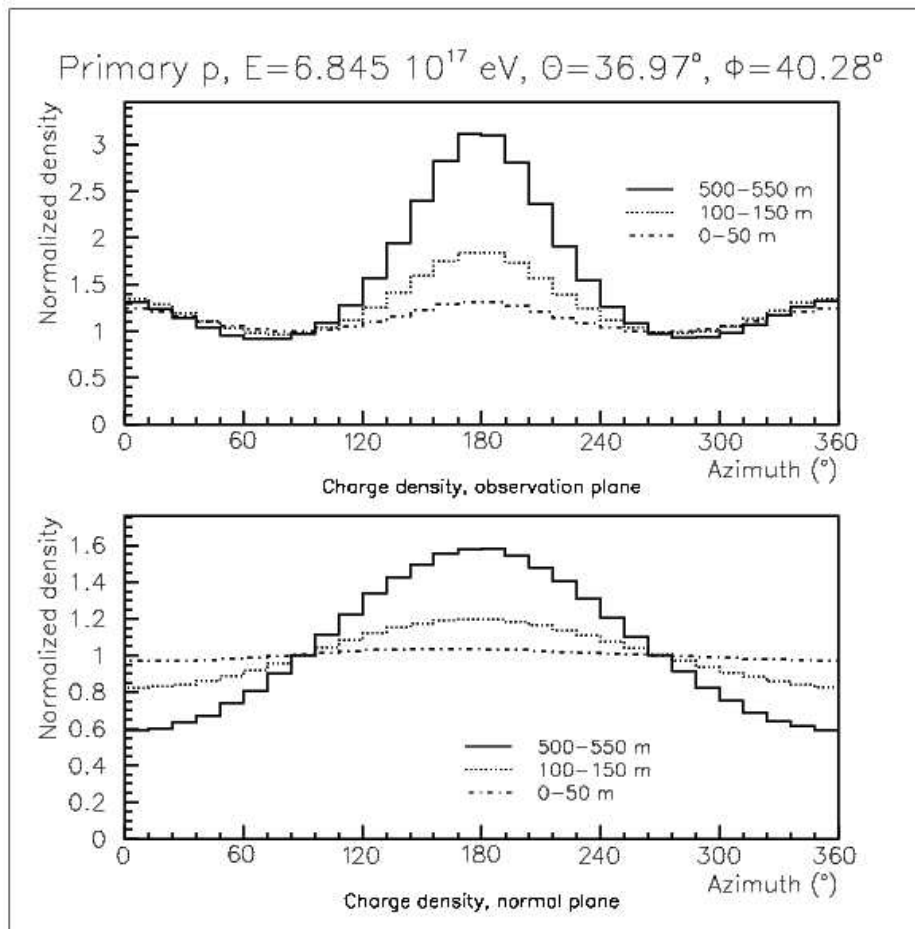The following figures (Figs. 5-11) display a selection of results, mainly for the primary

Figure 4: *The azimuthal distributions of the normalised charged particle density of high energy proton induced EAS in the observation plane and in the plane normal to the shower axis, displaying the variation with the azimuth ϕ.*

energy of 10^{15} eV, since the EAS of that energy have a muon content large enough leading to a sufficient statistical accuracy. Only the case of protons is displayed as primary Fe show similar features (see appendix). The distributions are displayed only in the observation plane as function of the azimuth angle ϕ around the shower core (with a changed definition of the azimuth angle different from the intrinsic coordinates used in Fig.4 with the further on convention: a point located in the North from the shower centre has azimuth ϕ = 0°, a point located in East has ϕ = 90°). Further cases are illustrated by the figures shown in the appendix.

The features shown in Figs. 5-11 can be understood when taking into account the direction of the geomagnetic vector (for the location of Karlsruhe for which the calculations are made, the magnetic inclination has a value of c.65° *North*, i.e. the vector points downwards).

Fig. 4 shows the azimuthal variation of the total charge particle component of proton induced showers of higher primary energy. Though the effect of the geomagnetic field is included, it is obscured since positive and negative particles behave in an opposite way, and since in addition the effect for electron and positrons appears to be less pronounced. The electrons and positrons considerably suffer from scatterings, changing the directions of the
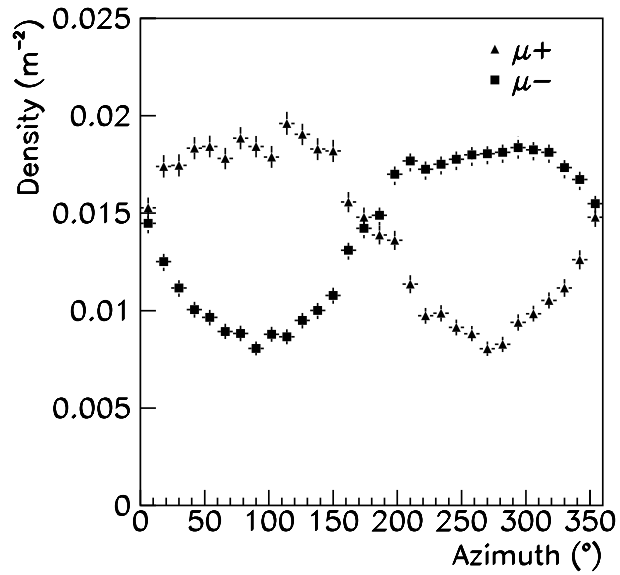
Figure 5: *The mean azimuthal μ^+- and μ^--distributions of proton induced EAS of inclined showers ($\theta = 45°$) incident from North with the primary energy of $10^{15}eV$ at a distance of $45 - 50\,m$ from the shower axis.*
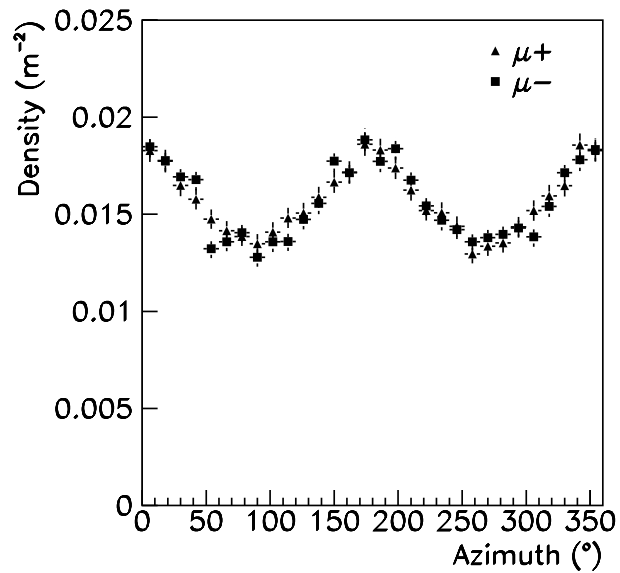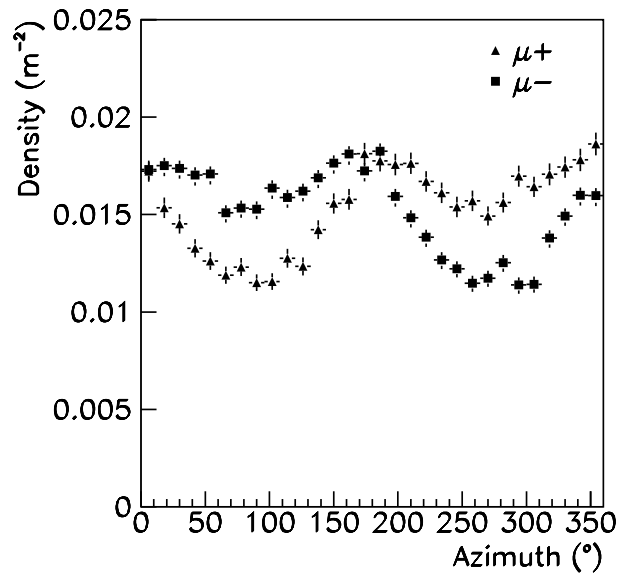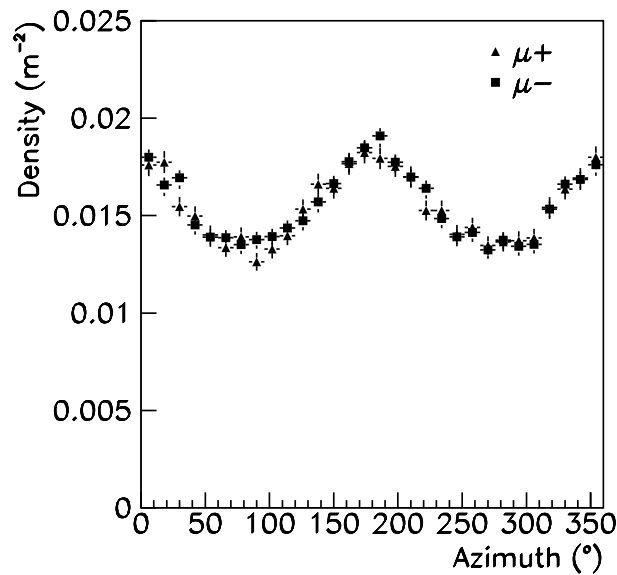

Figure 6: *The mean azimuthal μ^+- and μ^--distributions of proton induced EAS of inclined showers ($\theta = 45°$) incident from North with the primary energy of $10^{15}eV$ at a distance of $45 - 50\,m$ from the shower axis. Earth's magnetic field switched off.*
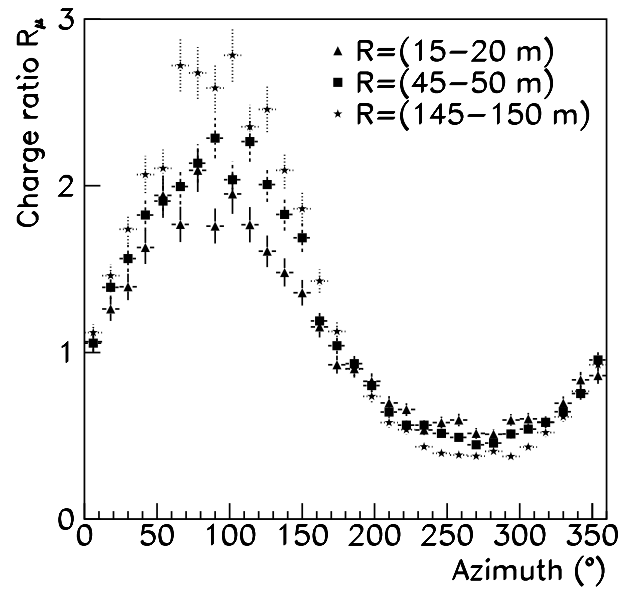
Figure 7: *The mean azimuthal μ^+- and μ^--distributions of proton induced EAS of inclined showers ($\theta = 45°$) incident from South with the primary energy of $10^{15} eV$ at a distance of $45 - 50\,m$ from the shower axis.*

Figure 8: *The mean azimuthal μ^+- and μ^--distributions of proton induced EAS of inclined showers ($\theta = 45°$) incident from South with the primary energy of $10^{15} eV$ at a distance of $45 - 50\,m$ from the shower axis. Earth's magnetic field switched off.*

Figure 9: *Variation of the charge ratio R_μ of the mean muon density distribution of proton induced EAS of inclined showers ($\theta = 45°$) incident from North with the primary energy of $10^{15} eV$ at various distances R from the shower axis.*

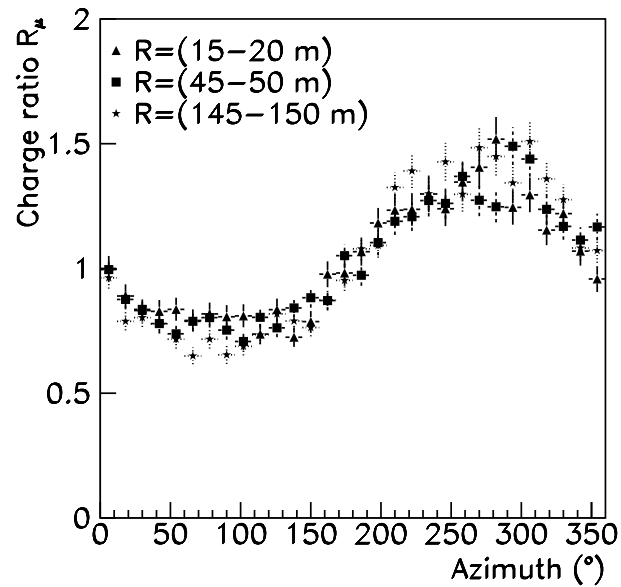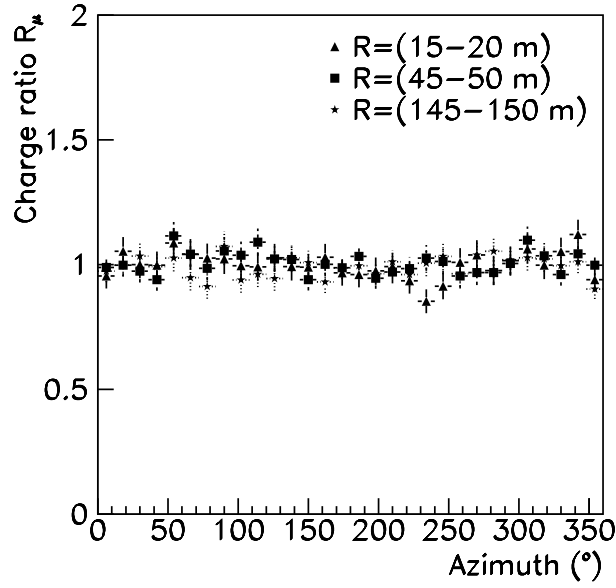Figure 10: *Variation of charge ratio R_μ of the mean muon density distribution of proton induced EAS of inclined showers ($\theta = 45°$) incident from South with the primary energy of $10^{15} eV$ at various distances R from the shower axis.*

Figure 11: *Variation of charge ratio R_μ of the mean muon density distribution of proton induced EAS of inclined showers ($\theta = 45°$) incident from North with the primary energy of $10^{15} eV$ at various distances R from the shower axis. Earth's magnetic field switched off.*

momenta relative to the geomagnetic field.

Hence the total charge particle distribution resembles the μ^+- and μ^--distributions, (where the geomagnetic influence is very distinct in the realistic case, see Fig. 5), when the geomagnetic field is just "switched off" (Fig. 6). For more details about the influence of the Earth's magnetic field on the electron component, see the Figs. 28-31 at the appendix!

In Fig. 5 the particles are coming from the North. Thus the Lorentz force acting on the path ways of μ^+ is directed towards East and the μ^+-density is enhanced around 90° (East). In case the particles are coming from South, the Lorentz force acts on μ^+ in the opposite direction, shifting the maximum of the distribution to West (Fig.7). However, quantitatively the effect of the Earth magnetic field is different for muons coming from North and South, respectively, for EAS of the same kind. This is due to the magnetic inclination of geomagnetic field, whose value for the location of Karlsruhe is $\gamma \approx 65°$, with the magnetic field pointing downwards. Thus the relative angle (geomagnetic angle) between the particle momenta ($\Theta = 45°$) and the magnetic vector amounts to be about 70° for particles from North, while for particles arriving from the South the value of the geomagnetic angle is 20°. This situation explains the different amplitudes of the azimuthal variation of the charge ratio in Figs. 9 and 10.

The azimuthal μ^+- and μ^--distributions, calculated with the geomagnetic field "switched off" and displayed in the observation plane, shown in Fig 6, are mainly the results of geometric effects. The density at $\phi = 0$ and $\phi = 180°$ is larger than at $\phi = 90°$ and $\phi = 270°$ since for density at the radial distance R from the shower center in the observation plane corresponds to the density at the radial distance $R \cdot \cos(\Theta)$ in the normal plane at $\phi = 0$ and $\phi = 180°$, but that at R for $\phi = 90°$ and $\phi = 270°$. The observation that the density at $\phi = 0$ and $\phi = 180°$ are practically identical indicates that the attenuation of the particle density is of minor importance for the muon distribution in the distance $R = 45 - 50$ m. At larger distances also attenuation effects get evident.

When increasing the distance from the shower core, the amplitude of the azimuthal variation of charge ratio (Figs.9 and 10) is increasing. This is due to the distortion of the lateral distribution, noticeably with increasing radial distance. For EAS arriving from the North the μ^+ density get shifted to larger distances from the shower center in East direction, i.e the density corresponds to the density of smaller radii of the undisturbed lateral distribution. In case of μ^- density corresponds there to the undisturbed lateral distribution of larger distances. For EAS arriving from South this happens in West direction. There are experimental observations [37] of the KASCADE-Grande experiment [33] which indicate similar features.

From these features and from tentative results of studies at lower primary energies we deduce the following conclusions:

1. The azimuthal variation of the muon density and of local muon charge ratio in EAS are strongly influenced at the considered energies by the geomagnetic field (compare Fig. 5 and Fig. 9).

2. This influence depends from the azimuthal direction of the EAS incidence, i.e the direction relative to the direction of the Earth magnetic field and it increases with the distance from the shower axis (compare Fig. 9 and Fig. 10).

3. In case of neglect of the geomagnetic field the azimuthal variation in the observation plane reduces to the variation due to geometry effects and for larger radial distances from the core also due to the attenuation effect (see Fig. 4) which does not influence differently positive and negative muons (consequently the integrated value of R_μ remains nearby unity, since obviously differences in the π^+ and π^- production remain rather small at the considered muon energies; see Fig. 11).

It should be additionally remarked that for proton induced showers (incident from North or South) the muon charge ratio, integrated over all distances results in $R_\mu = 1.028 \pm 0.002$ (for Fe induced EAS in $R_\mu = 1.025 \pm 0.0015$), where the uncertainty is the standard error for a typical EAS.

5 Influence of the EAS muon energy

The energy spectrum of EAS muons has a rather flat maximum at energies of some few GeV, before decreasing, say from 2-3 GeV on. Consequently, the features shown for a muon energy threshold of 0.1 GeV do not change very much when increasing the threshold to 1 GeV, at least not for the considered central range of radial distances from the shower center, since the fraction of muons below 1 GeV is only in the order of 10%. The features appearing when muons with energies larger than 10 and 100 GeV, respectively, are considered, are shown in Figs. 12 and 13 for the case of EAS arriving from the North.
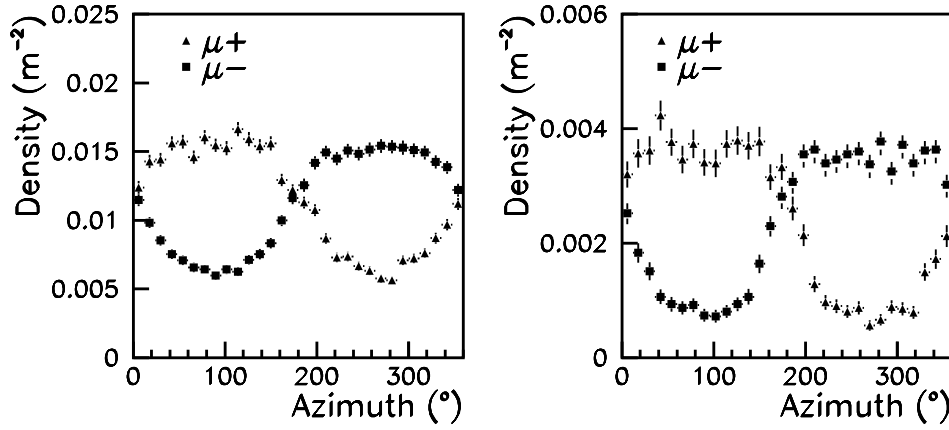
Figure 12: *The mean azimuthal μ^+- and μ^--distributions of proton induced EAS of inclined showers ($\Theta = 45°$) incident from North with the primary energy of 10^{15} eV at a distance of $45 - 50\,m$ from the shower axis: Comparison of different muon energy thresholds: 10 GeV (left) and 100 GeV (right).*
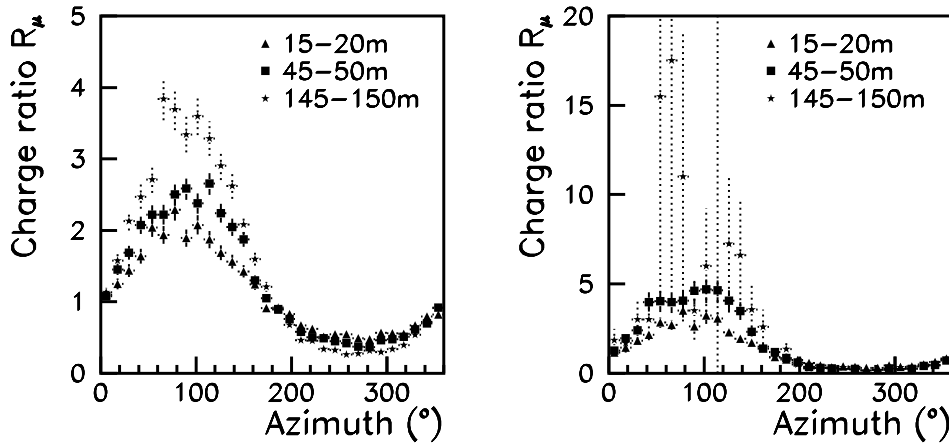

Figure 13: *Variation of the charge ratio R_μ of the mean muon density distribution of proton induced EAS of inclined showers ($\Theta = 45°$) incident from North with the primary energy of 10^{15} eV at various distances from the shower axis: Comparison of different muon energy thresholds: 10 GeV (left) and 100 GeV (right).*

The graphs which can be compared with Figs. 5 and 9 indicate also the strong decrease of the muon density with increasing the muon energy beyond few GeV. This does cast some doubt on the practicability of attempts to use the Earth magnetic field as charge separator of

TeV muons of very inclined EAS [29,30]. The variation of the muon charge ratio, though globally with the same features like at lower energies, displays increasing amplitudes with increasing the muon energy.

6 Remarks on similar features of radio emission from EAS

The electromagnetic component of extended air showers is accompanied by various types of secondary radiation arising from different interaction mechanisms. Recently the emission of radiation in the radio frequency range ("radio flashes") from EAS has been rediscovered [38], which most likely originates from the so called coherent geosynchrotron effect: electron positron pairs get bent in the terrestrial magnetic field and are emitting synchrotron radiation. This discovery, already indicated by early observations in the sixties, recently definitively confirmed by the advanced detection techniques, has prompted considerable activities, e.g. the installation of LOPES [39]. That is an array of a number of dipole antennas placed inside the particle detector array of KASCADE-Grande for the detection of radio emission in coincidence with air showers observed with particle detectors. According to analytical studies [40] a broadband short radio pulse in the nanosecond range is expected, observable on ground with $5 - 15$ V/m/MHz for EAS of the energy range of 10^{17} eV. In fact such radio pulses have been observed with the digital radio antenna field of thirty East-West polarised short antennas located within the KASCADE-Grande field.
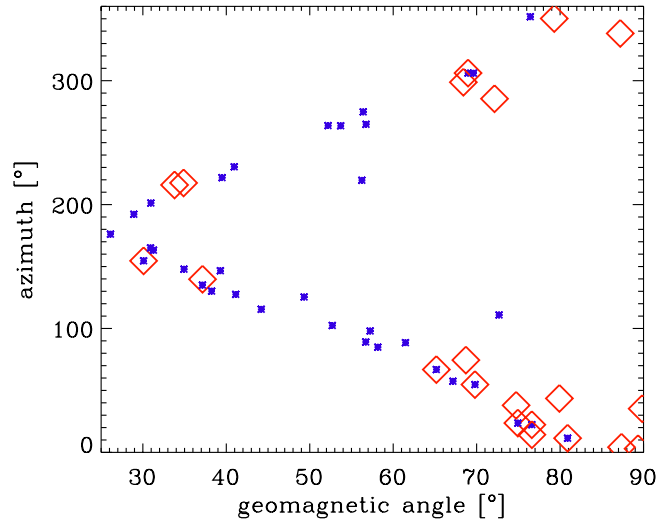

Figure 14: *Inclined EAS as a function of azimuth and geomagnetic angles [43]. Crosses represent events which are reconstructed from KASCADE-Grande observations, rhombs indicate events detected by radio signals. The azimuth convention is the same as in previous graphs: $90°$ and $270°$ azimuth angles denote showers coming from East and West, respectively, $180°$ and $0/360°$ denote showers arriving from South and North, respectively.*

The assumed geomagnetic origin of the expected emission process suggests a dependence of the resulting field strength at observation position on the direction of the terrestrial magnetic field like the effects of the geomagnetic field on the variation of the EAS muon density. Indeed, a $1 - \cos\gamma$ correlation of the field strength with the angle between Earth magnetic field and shower axis (geomagnetic angle γ) was found [38]. But following simulation studies, the dependence on the strength and geometry of the magnetic field appears to be more subtle than intuitively expected, and detailed effects s how up in the polarisation characteristics of the radio signal. Simulations [41] let expect that the emission and the radio signal strength - like the EAS muon density - depend as well on the zenith as on the azimuth angles and not simply only on the geomagnetic angle. Thus inclined showers with large zenith angles exhibit a much larger radio footprint at observation level, making them especially favourable for radio detection. This feature is analogous to the separability of positive and negative muons by the Earths magnetic field with increasing zenith angle. The

azimuthal angle, which is of course related with geomagnetic angle γ at a given observation location and zenith angle of EAS incidence, defines the degree of the polarization of the measurable signal. In addition to the zenithal shower direction also the (azimuthal) position of the observer influences the field strength and the degree of polarization [42].

It is of interest to compare the azimuthal dependence of the radio signal with the dependence of the muon charge ratio from the azimuthal incidence. The muon charge ratio provides a measure of the separation of positive and negative charges by the geomagnetic field. The present experimental status of information from LOPES is displayed in Fig. 14, where a sample of observed showers with zenith angle of incidence larger than $50°$ is shown. Large zenith angles are considered, not only because of the enhanced appearance of radio signals, but also since a larger range of the geomagnetic angle values could be covered. The graph [43] shows KASCADE-Grande triggered and radio detected events in a plot of azimuth angle of incidence vs. the geomagnetic angle. Two features can be noticed:

- A pronounced North-South asymmetry. There appear more detected events arriving from the North than from the South, which is probably related to the fact that cosmic rays arriving from North have the largest geomagnetic angles. This feature is analogous to the different amplitudes of the azimuthal variation of the muon charge ratio for EAS arriving from North and from South (see Figs. 9 and 10).

- A pronounced gap with no detected radio events (missing "rhombs" region in Fig. 14). There appear no radio signals from showers coming from East or West ($90°$ and $270°$). This may be explained by the fact that the particular antenna arrangement of LOPES used at that time did only measure the East-West linear polarisation of the radiation. Simulations predict that the radio waves from showers arriving from East or West should be mostly North-South polarised. This effect of the polarisation has of course no analogon in the variation of the muon density.

Obviously the influence of the Earth's magnetic field plays in both cases a dominant role for detailed features of the μ^+ and μ^- density distributions and of the emission of the radio waves from EAS.

7 Concept of experimental approaches

Experimental studies of the azimuthal and radial variations of the charge ratio of the muon density in EAS would need a device (spectrometer) for the determination of R_μ placed inside or nearby a detector array for determining the incident EAS, the direction of incidence, defining also the azimuth position (relative to the plane of shower incidence) of the spectrometer and the position of the shower core relative to the location of the spectrometer.

The group of the Okayama University, Japan [44,45] has installed on the rooftop of a campus building a small array of 8 plastic scintillators (OU array) scintillators (OU array) to observe extensive air showers. In addition there is a magnetic spectrometer (Okayama telescope) located below the OU array to spectroscopy positive and negative muons, especially to determine the charge sign from the curvature of the tracks of the incident muons and the charge excess of the muons with a momentum larger than 1 GeV/c. The apparatus could be used for coincidence observation of the EAS array with the magnetic spectrometer. First results of the analyses of measured data indicate a charge excess, disappearing within the (large) error bars. But there has been neither the azimuth location of the spectrometer relative to the shower plane nor the angles of the incident EAS specified, and the results may be understood as an average canceling out the effects. Also the fact that the Okayama telescope finds a rather small value of the muon charge ratio of atmospheric muons may cast some doubts on the systematic accuracy of the measurements.
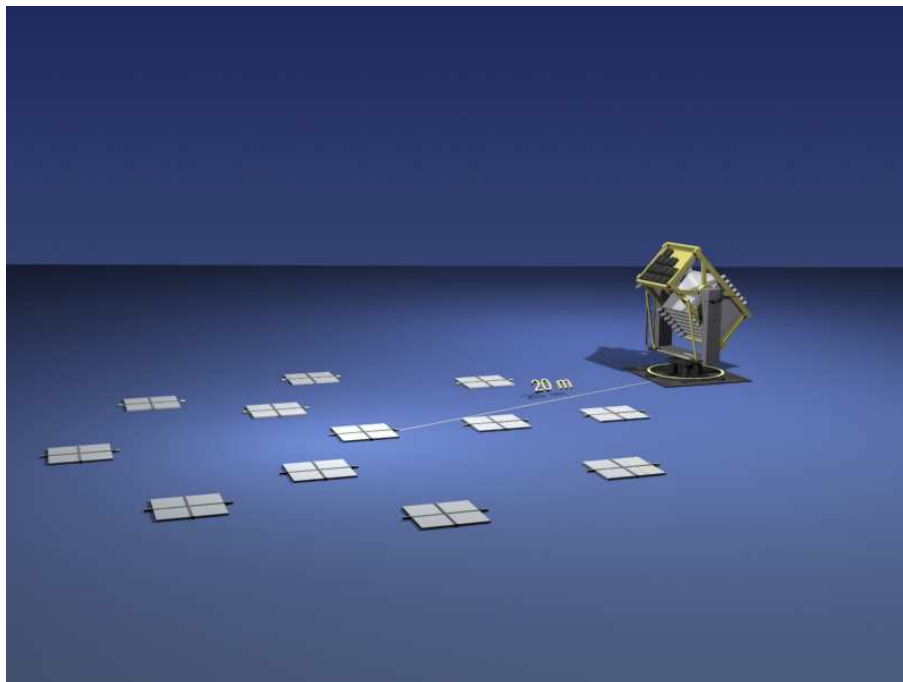

Figure 15: *Sketch of the geometrical layout of a mini-array for triggering the nearby located WILLI device for muon detection [28].*

The spectrometer WILLI [2,46,28] installed in Bucharest, Romania determines the muon charge ratio by measuring the life time of the muons stopped in a stack of 16 detector layers. The life time is different for positive and negative muons as negative muons can be captured in atomic orbits, thus leading to an effectively reduced lifetime, depending on the stopping material. The uncertainties of the efficiencies for the detection of differently charged muons and of the geometrical acceptance, usually affecting magnetic

spectrometers, are canceled out. The detector area of the device is able to be directed in
a particular direction to measure the incoming muons under different (zenith and azimuth)
angles of incidence. Actually WILLI has provided results of successful measurements, re-
sulting in R_μ-values well in the range of the world average, down to a momentum range
of about $0.2\,$MeV/c. It has demonstrated the azimuthal variation (East-West effect) of the
muon charge ratio of atmospheric muons.

There is a proposal (see ref. [28]) to equip the WILLI device with an array of 12 scin-
tillator units, located nearby WILLI, in order to determine the EAS core position relative
to the WILLI device and the direction of incidence of showers of the energy region of
$10^{14} - 10^{15}\,$eV, providing a trigger for WILLI. Fig. 15 displays a sketch of a geometri-
cal layout of the detector system which is under consideration by simulation studies with
respect to the efficiency and the detector responses. Though such a small array will not
be able to determine the energy of the incident showers, it is expected that such detector
system will provide more detailed information about the different propagation of positive
and negative EAS muons, in particular under the influence of the geomagnetic field.

8   Concluding remarks

EAS simulations show that the lateral density distributions of the positive and negative muons are varying not only with the (radial) distance from the shower axis, but also with the azimuth relative to the plane of the incident shower. The reasons are different. In addition to the attenuation effects of charged particles of inclined showers [15] in the atmosphere by the variation of the travelling distances in the atmosphere, the geomagnetic field affects the travel of positive and negative muons in an opposite way. The geomagnetic effects depend on the direction of the EAS axis relative to the Earths magnetic vector. This leads to an azimuthal variation of the muon charge ratio of the muon density distribution. In the extreme case of very inclined showers (with long slant depths) the Earth field might be used as magnetic separator [29,30]. Obviously the experimental detection of these features is of great interest for the understanding of the EAS development. Furthermore the quantitative results would also provide some information about the hadronic interaction, in particular when observing higher energy muons (see [20]). The aspect of the dependence on the hadronic interaction models, currently en vogue [47], has not been systematically explored in the present paper.

References

[1] J. Wentz et al., J. Phys. G: Nucl. Part. Phys. 27 (2001) 1699;
    J. Wentz et al., Phys. Rev. D 67 (2003) 073020.

[2] B. Vulpescu et al., Nucl. Instr. Methods A 414 (1998) 205;
    B. Vulpescu et al., J. Phys. G Nucl. Part. Phys. 27 (2001) 977.

[3] R.K. Adair et al., Phys. Rev. Lett. 39 (1977) 112;
    W.Y. Hwang and B.Q. Ma, Eur. Phys. Journ. A 25 (2005) 467.

[4] Y. Fukuda et al ., Phys. Rev. Lett. 81 (1998) 1562.

[5] Q.R. Ahmad et al., Phys. Rev. Lett. 89 (2002) 011301.

[6] P. Lipari, Astropart. Phys. 14 (2000) 171.

[7] P. Lipari, T. Stanev and T.K. Gaisser, Phys. Rev. D 58 (1998) 073003.;
    P. Lipari and T. Stanev, Proc. 24th ICRC 1995, Rome, Italy, vol.1 p.516.

[8] T.H. Johnson, Phys. Rev. 43 (1933) 307; ibid 43 (1933) 381; ibid 48 (1935) 287;
    see also B. Rossi, CosmicRays, (McGraw-Hill, New York 1964).

[9] P.K.F. Grieder, Cosmic Rays on Earth, Researcher's Reference Manual and Data
    Book (Elsevier, Amsterdam 2001)

[10] P. Lipari, Astropart. Phys. 1 (1993) 195

[11] T. Hebbeker and C. Timmermans, Astropart. Phys. 18 (2002) 107

[12] S. Coutu et al., Proc. ICHEP 98 Vancouver, Canada 1 (1998) 666

[13] J. Kremer et al., Phys. Rev. Lett. 83 (1999) 4241

[14] M. Motoki et al Astropart. Phys. 19 (2003) 113

[15] A. Patrascioiu, O. Sima and H. Rebel, Internal Report KASCADE-Grande 2006-01
    Forschungszentrum Karlsruhe

[16] Andreas Haungs, Heinigerd Rebel and Markus Roth, Rep.Progr.Phys. 66 (2003) 1146

[17] T.K. Gaisser, Cosmic Rays and Particle Physics, Cambridge University Press, Cam-
    bridge MA 1990

[18] M.G. Thompson and M.R. Whalley , J. Phys.: Nucl. Phys. 3 (1977) 97

[19] D.P. Bhattacharyya and R.K.Roychoudhury, Aust. J. Phys 32 (1979) 369

[20] Michael Unger et al. - L3 Collaboration, Int. J. Mod. Phys. A 20 (2005) 6928

[21] D. Zimmermann et al. - Cosmo-Aleph Collaboration, 28th ICRC Tsukuba Japan,
    2003, vol 3, p.1183

[22] N.N. Kalmykov S. Ostapchenko and A.I. Pavlov, Nucl. Phys. B Proc. Suppl. 52 (1977)
    17

[23] R.S. Fletcher, T.K. Gaisser, P. Lipari and T. Stanev, Phys. Rev. D 50 (1994) 5710

[24] C. Störmer, Astrophysics 1 (1930) 237

[25] J. Wentz, A. Bercuci and B. Vulpescu, Proc. 27th ICRC, Hamburg 2001, vol 3, p.1167

[26] O.C. Allkofer et al., Journ. Geophys. Research 90 (1985) 3537

[27] T. Futagami et al. - Super-Kamiokande Collaboration, Phys. Rev. Lett. 82 (1999) 5194

[28] I.M. Brancus et al., Proc. ISVHECRI 2006, Weihei, China, Nucl. Phys. B (Suppl.), in press

[29] Bing Kan and Bo-Qiang Ma, [arXiv: astro-ph/0611717] 2006;

[30] M. Ave, R.A. Vasquez and E. Zas, Astropart. Phys. 14 (2000) 91

[31] J. Matthews, Astropart. Phys. 22 (2005) 387

[32] W. Heitler, The quantum theory of radiation, Oxford 1954

[33] A. Haungs et al.- KASCADE-Grande Collaboration, Proc. 28th ICRC 2003, Tsukuba, Japan, vol.2, p.985

[34] D. Heck et al., Report FZKA6019, Forschungszentrum Karlsruhe (1998)

[35] H. Fesefeldt, PITHA-85/02, RWTH Aachen

[36] W.R. Nelson, H. Hirayama and D.W. Rogers, Report SLAC 265, Stanford Linear Acelerator Center 1985

[37] R. Obenland, Report FZKA 7116, Forschungszentrum Karlsruhe (2005)

[38] H. Falcke et al. - LOPES collaboration, Nature 435 (2005), 313.

[39] A. Horneffer et al. - LOPES collaboration, Int Journal Mod Phys A 21 Suppl.1, (2006) 168

[40] T. Huege, H. Falcke, Astronomy & Astrophysics, 412 (2003) 19.

[41] T. Huege, H. Falcke, Astropart. Phys. 24 (2005) 116.

[42] T. Huege, R. Ulrich, R. Engel, Astropart. Phys. (2006), in press, astro-ph/0611742

[43] J. Petrovic et al. - LOPES collaboration, Astronomy & Astrophysics (2006), in press, astro-ph/0611225

[44] S. Tsuji et al. Proc. 29th ICRC 2005 Pune, India, vol 8, p.213

[45] S. Tsuji et al. Proc. 29th ICRC 2005 Pune, India, vol 6, p.233;
S. Tsuji et al. Proc. ISVHECRI 2006, Lisbon, Portugal, in press

[46] I.M. Brancus et al., Nucl. Phys. A721 (2003) 1044c;
I.M. Brancus et al., Proc. 10th International Conference on Nuclear Reaction Mechanism,Varenna, Italy 2003, Univ. Milano, p.645

[47] S. Ostapchenko [arXiv:astro-ph/06107788]2006; J. Phys. Conference Ser. 2007, in press

A   Appendix

This appendix displays results which detail the calculations of the mean azimuthal μ^+ and μ^- distributions and of the variation of the muon charge ratio in EAS, and they underline the above conclusions. The examples include the cases of EAS arriving from East and West, indicating the differences arising for different geomagnetic angles. In addition the case of Fe induced showers has been explored (Figs. 22,23,26,27), exhibiting qualitatively similar features.

Figs. 28-31 demonstrate the minor influence of the magnetic field on the dominating electron - positron EAS component though not completely negligible. The variation of the density can be directly compared with the results given in Figs 5 - 8. The variation of density distribution appears to be largely governed by the geometrical effects of the density of inclined showers, but also attenuation can be observed. Indeed while for EAS arriving from North the density in the "early" region ($\phi = 0$) is noticeably higher than in the "late" region ($\phi = 180°$), in case of EAS arriving from South the azimuth values of the "late" and "early" region are interchanged due to our definition used for the azimuth angle along the astronomical azimuth.

For the muon density distributions the attenuation is not significant.
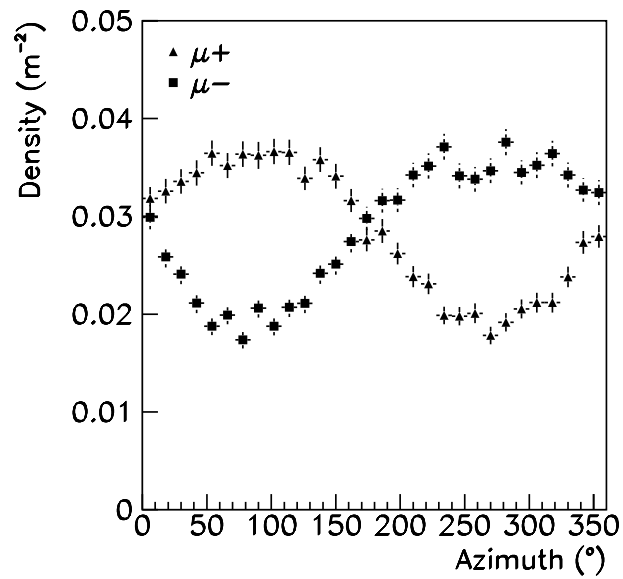
Figure 16: *The mean azimuthal μ^+ and μ^- distributions of* **proton** *induced EAS of inclined showers ($\Theta = 45°$) incident from* **North** *with the primary energy of 10^{15} eV at a distance of $15 - 20$ m from the shower axis.*
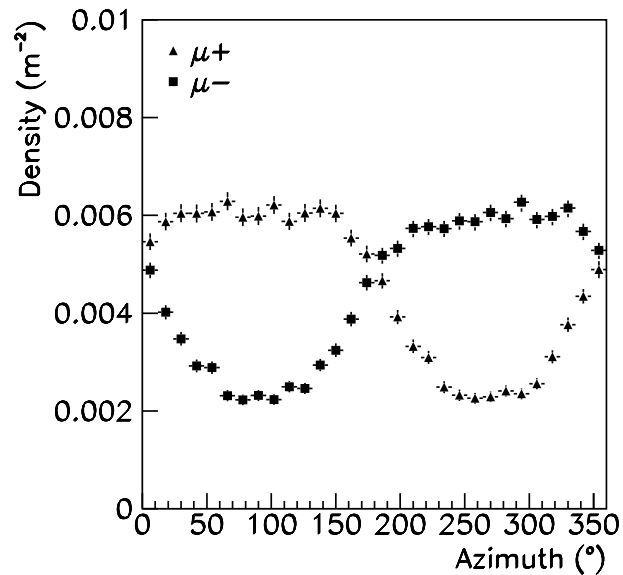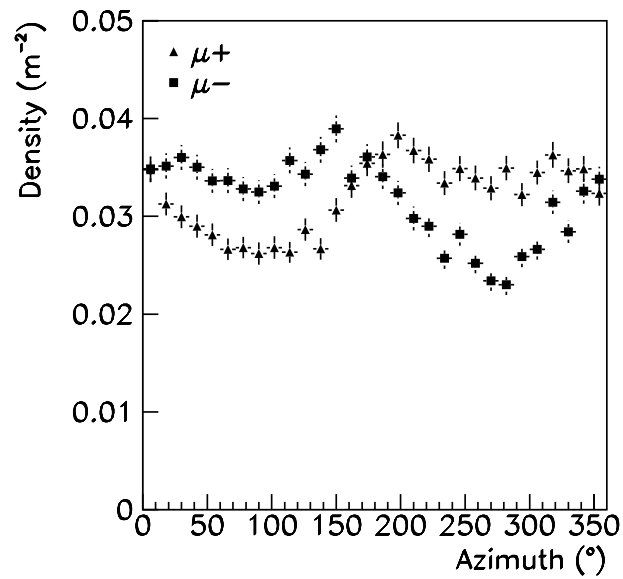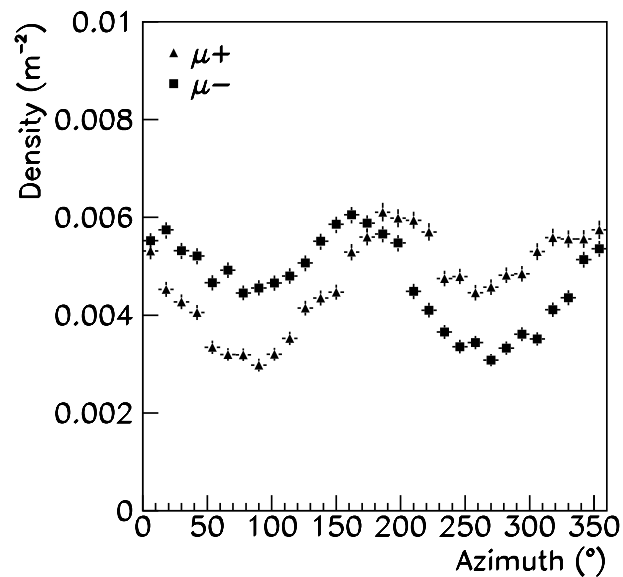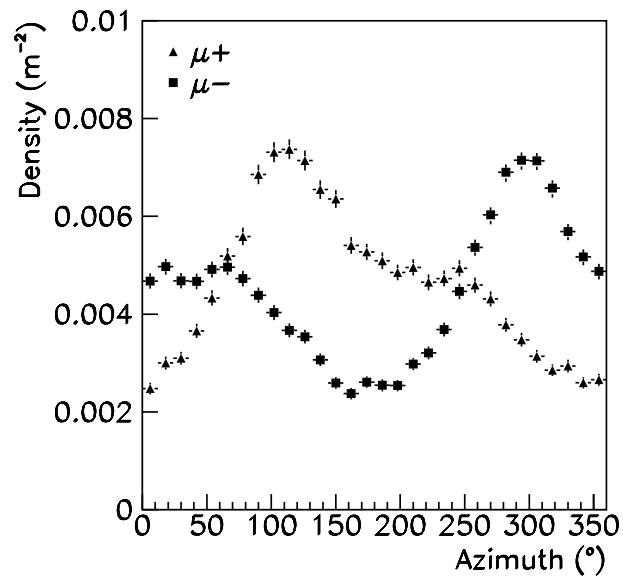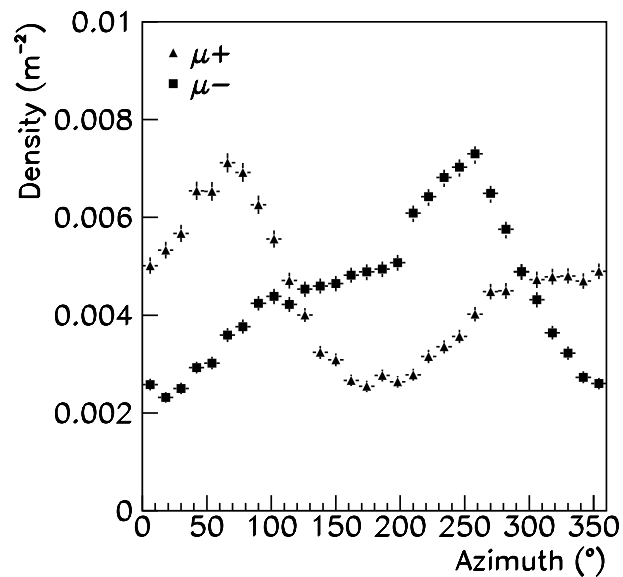

Figure 17: *The mean azimuthal μ^+ and μ^- distributions of* **proton** *induced EAS of inclined showers ($\Theta = 45°$) incident from* **North** *with the primary energy of 10^{15} eV at a distance of $145 - 150$ m from the shower axis.*
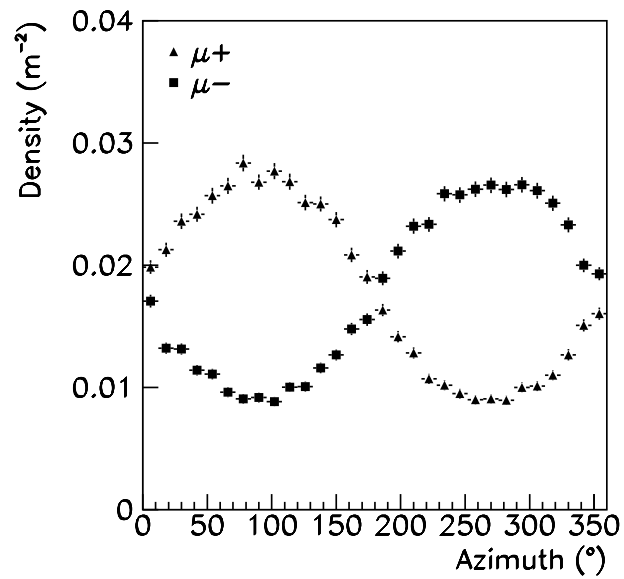
Figure 18: *The mean azimuthal μ^+ and μ^- distributions of* **proton** *induced EAS of inclined showers ($\Theta = 45°$) incident from* **South** *with the primary energy of $10^{15}\,eV$ at a distance of $15 - 20\,m$ from the shower axis.*
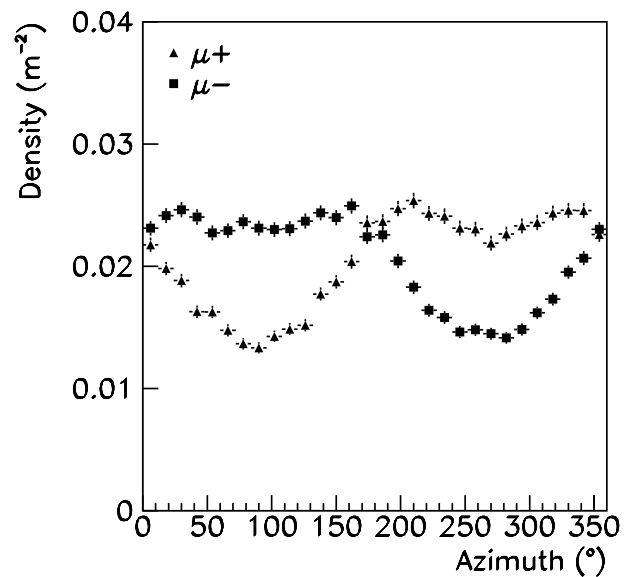

Figure 19: *The mean azimuthal μ^+ and μ^- distributions of* **proton** *induced EAS of inclined showers ($\Theta = 45°$) incident from* **South** *with the primary energy of $10^{15}\,eV$ at a distance of $145 - 150\,m$ from the shower axis.*

Figure 20: *The mean azimuthal μ^+ and μ^- distributions of* **proton** *induced EAS of inclined showers ($\Theta = 45°$) incident from* **East** *with the primary energy of $10^{15}\,eV$ at a distance of $145 - 150\,m$ from the shower axis.*
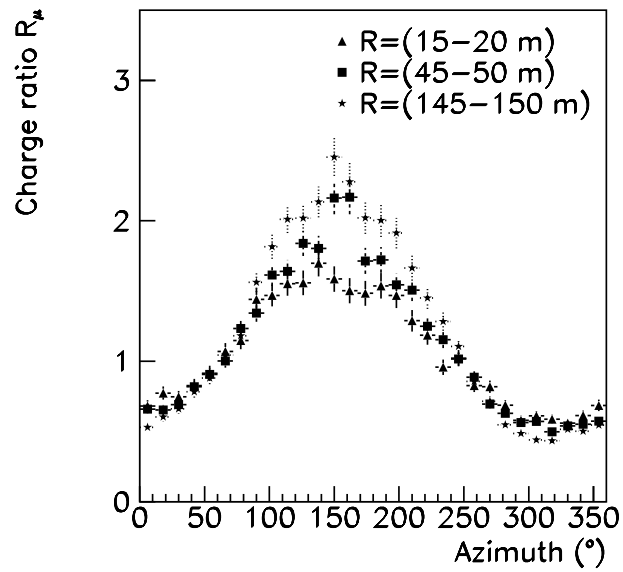

Figure 21: *The mean azimuthal μ^+ and μ^- distributions of* **proton** *induced EAS of inclined showers ($\Theta = 45°$) incident from* **West** *with the primary energy of $10^{15}\,eV$ at a distance of $145 - 150\,m$ from the shower axis.*

Figure 22: *The mean azimuthal μ^+ and μ^- distributions of* **iron** *induced EAS of inclined showers ($\Theta = 45°$) incident from* **North** *with the primary energy of 10^{15} eV at a distance of $45 - 50$ m from the shower axis.*

Figure 23: *The mean azimuthal μ^+ and μ^- distributions of* **iron** *induced EAS of inclined showers ($\Theta = 45°$) incident from* **South** *with the primary energy of 10^{15} eV at a distance of $45 - 50$ m from the shower axis.*

Figure 24: *Variation of charge ratio R_μ of the muon density distribution of* **proton** *induced EAS of inclined showers ($\Theta = 45°$) incident from* **East** *with the primary energy of $10^{15}\,eV$ at various distances from the shower axis.*
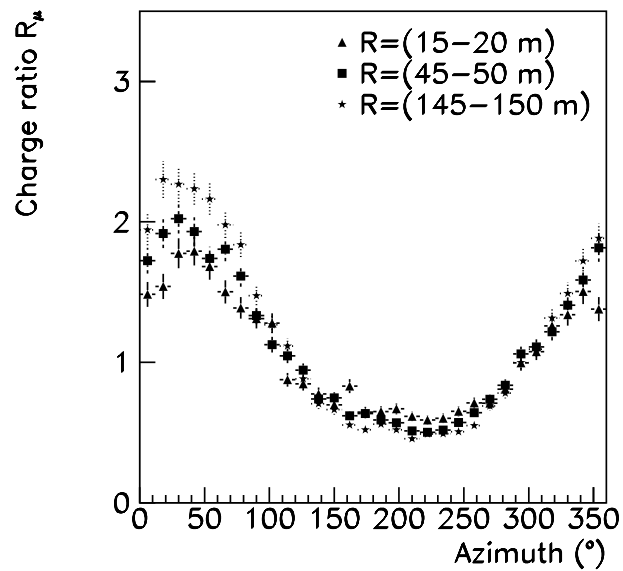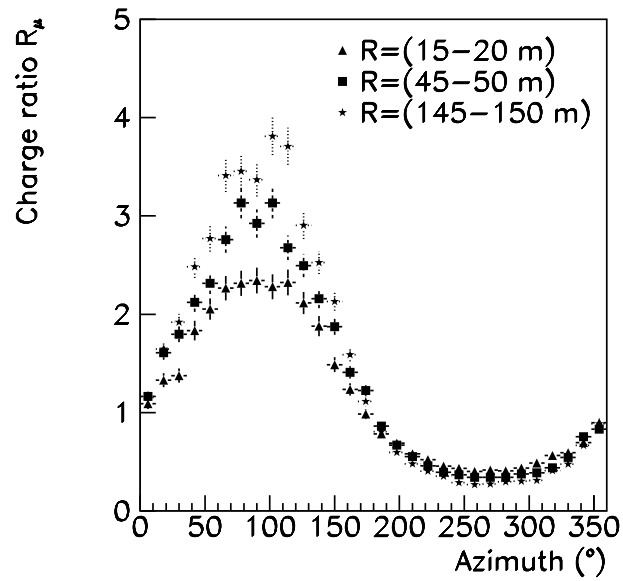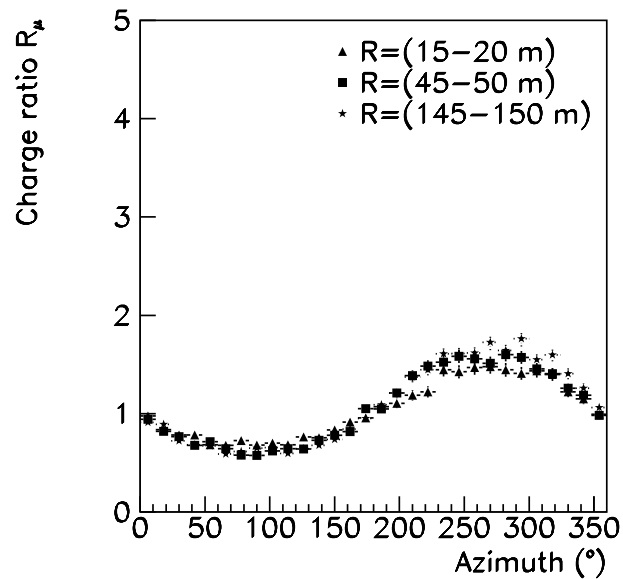

Figure 25: *Variation of charge ratio R_μ of the muon density distribution of* **proton** *induced EAS of inclined showers ($\Theta = 45°$) incident from* **West** *with the primary energy of $10^{15}\,eV$ at various distances from the shower axis.*

Figure 26: *Variation of charge ratio R_μ of the muon density distribution of* **iron** *induced EAS of inclined showers ($\Theta = 45°$) incident from* **North** *with the primary energy of* $10^{15}\,eV$ *at various distances from the shower axis.*

Figure 27: *Variation of charge ratio R_μ of the muon density distribution of* **iron** *induced EAS of inclined showers ($\Theta = 45°$) incident from* **South** *with the primary energy of* $10^{15}\,eV$ *at various distances from the shower axis.*
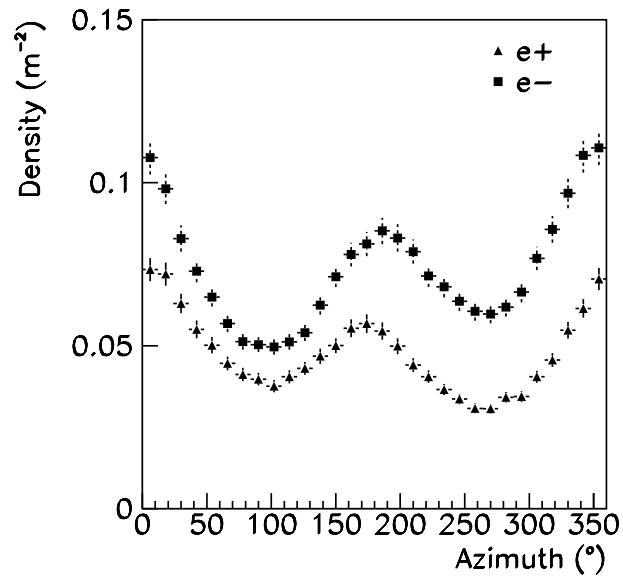
Figure 28: *Azimuthal variation of the* **electron** *density distribution in the distance of 45 − 50 m from the core for proton induced EAS (*10^{15} *eV) incident from* **North***.*
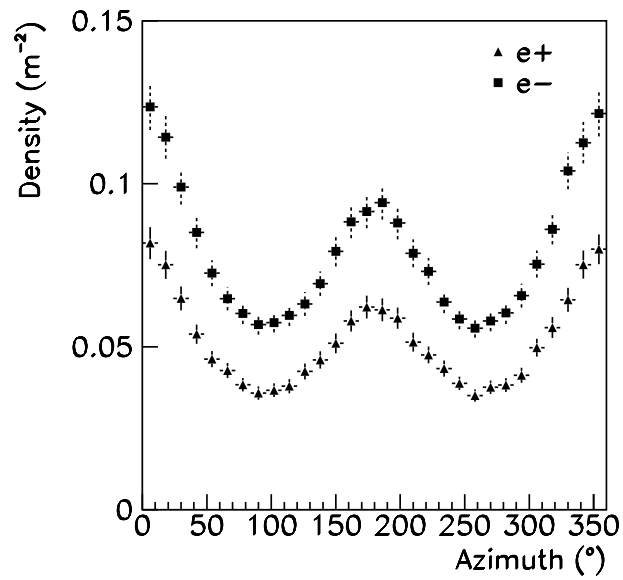

Figure 29: *Azimuthal variation of the* **electron** *density distribution in the distance of 45 − 50 m from the core for proton induced EAS (*10^{15} *eV) incident from* **North***, with the influence of the geomagnetic field switched off.*
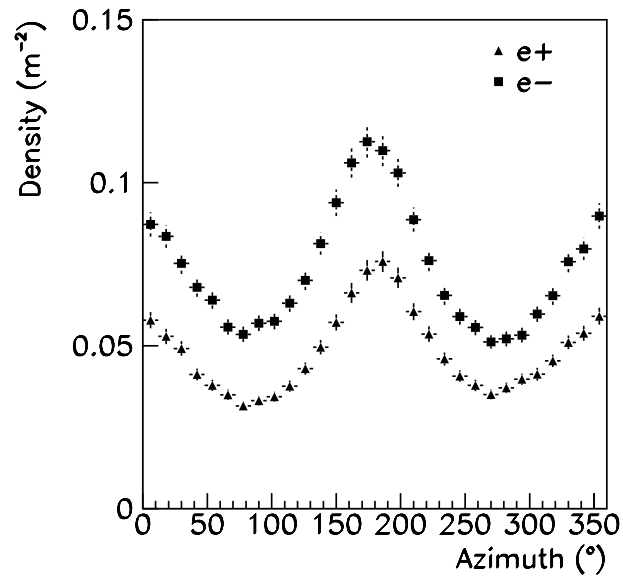
Figure 30: *Azimuthal variation of the* **electron** *density distribution in the distance of* 45 − 50 *m from the core for proton induced EAS (*10^{15} *eV) incident from* **South**.
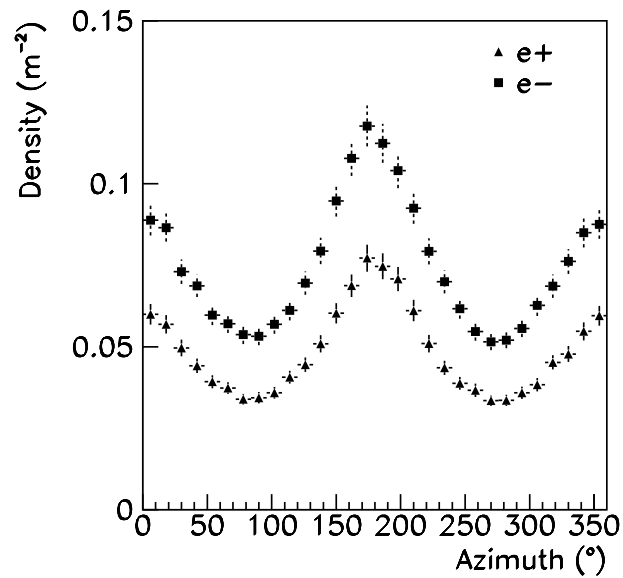

Figure 31: *Azimuthal variation of the* **electron** *density distribution in the distance of* 45 − 50 *m from the core for proton induced EAS (*10^{15} *eV) incident from* **South**, *with the influence of the geomagnetic field switched off.*